

Article

Age of Information and Success Probability Analysis in Hybrid Spectrum Access-Based Massive Cognitive Radio Networks

Samuel D. Okegbile *  and Bodhaswar T. Maharaj 

Department of Electrical, Electronic and Computer Engineering, University of Pretoria, Hatfield, Pretoria 0002, South Africa

* Correspondence: samokegbile@gmail.com

Abstract: In this paper, we investigate users' performance under the hybrid spectrum access model in the massive cognitive radio network (CRN), where multiple primary users (PUs) and secondary users (SUs) transmit on the same channel simultaneously. SUs first detect the state of the channel via channel sensing and select an appropriate channel access scheme (either underlay or overlay) for their transmissions based on the outcome of the channel sensing. When at least one PU is active, SUs transmit under the underlay channel access scheme by employing the power control technique to ensure that the interference generated in the primary network is below the pre-defined interference threshold. In the absence of PU, SUs transmit with full transmit power under the overlay channel access scheme, thereby maximizing their throughput. Using the tool of stochastic geometry, we obtained tractable analyses for important metrics such as success probability, throughput, and the average age of information (AoI) in both primary and secondary networks, while capturing the interference between the two networks. The obtained analyses offer an efficient way to understand the metrics of AoI, throughput and success probability in the hybrid spectrum access-based CRN. We further compared users' performance under the hybrid spectrum access scheme with performances under overlay and underlay spectrum access schemes. The outcome of the numerical simulations shows that the hybrid spectrum access scheme can significantly improve the performance of users in the network, while also capturing more key features of real-life systems.

Keywords: age of information; cognitive radio; hybrid spectrum access model; stochastic geometry; throughput



Citation: Okegbile, S.D.; Maharaj, B.T. Age of Information and Success Probability Analysis in Hybrid Spectrum Access-Based Massive Cognitive Radio Networks. *Appl. Sci.* **2021**, *11*, 1940. <https://doi.org/10.3390/app11041940>

Academic Editor: Jozsef Katona

Received: 4 November 2020

Accepted: 17 January 2021

Published: 23 February 2021

Publisher's Note: MDPI stays neutral with regard to jurisdictional claims in published maps and institutional affiliations.



Copyright: © 2021 by the authors. Licensee MDPI, Basel, Switzerland. This article is an open access article distributed under the terms and conditions of the Creative Commons Attribution (CC BY) license (<https://creativecommons.org/licenses/by/4.0/>).

1. Introduction

The continuous proliferation of wireless communications systems and services implies that the subject of spectrum management and availability continue to attract attentions. In fact, over 25 billion devices are expected to be connected on the internet by the year 2025. A successful communication among these devices requires proper coordination among users on the scarce spectrum resources; hence, investigating the behaviour and performance of users in the cognitive wireless communications networks is a necessity.

1.1. Hybrid Spectrum Access

One important paradigm that has been successful in managing the usage of spectral resources is the cognitive radio network (CRN). In CRN, unlicensed devices, known as secondary users (SUs), are allowed to transmit on channels belonging to licensed users—known as primary users (PUs)—as long as the transmissions of SUs do not cause a disruptive interference to the activities or transmissions of PUs. In order to ensure that the quality of service (QoS) of PUs is not affected, while ensuring an improved throughput and channel usage experience for SUs, channel access in CRN is often managed under three popular paradigms—underlay, overlay and hybrid channel access models, depending on the channel access relationship between PUs and SUs [1]. For the sake of convenience, we used the terms model, mode and scheme interchangeably throughout this paper.

In the overlay channel access scheme, SUs are not allowed to transmit in the presence of PUs and must regularly perform channel sensing to determine the state of the channel [2]. If the outcome of the channel sensing indicates the presence of at least one PU on any typical channel, no SU is allowed to access such a channel for transmissions. SUs must, therefore, wait until such a channel is idle or can switch to any other idle channel via the channel switching process. Hence, interference resulting from the activities of SUs at the PUs in the overlay channel access scheme depends on the sensing accuracy level of SUs. Although interference in the overlay channel access scheme can be significantly controlled and reduced, it may be difficult to satisfy SUs' spectrum access requirements, especially on channels with the dominant presence of PUs, since SUs must always vacate the band before the arrival of PUs on such channels.

The underlay spectrum access scheme, on the other hand, allows SUs to transmit on channels belonging to PUs at any time, provided that the interference received at any tagged PU is below the pre-defined maximum allowable interference level—known as interference temperature. Hence, SUs are expected to adopt appropriate power control techniques during transmissions. The need to adopt adequate power control techniques in the underlay model, however, means that the underlay spectrum access CRN is a more aggressive spectrum access technique [1]. The last paradigm is the hybrid model which combines the uniqueness of both the underlay and overlay models. The hybrid spectrum access model has, however, received less attention because of the difficulty in obtaining various analyses of interest for such a model.

The hybrid spectrum access mechanism permits SUs' transmissions in both the overlay and underlay schemes depending on the state of the channel [1,3] and has been receiving attention recently owing to the need to compare its performance and demonstrate its advantages over the conventional underlay and overlay spectrum access models. In the hybrid model, SUs must carry out regular channel sensing for effective detection of PUs' channel information. Each SU must then select an appropriate channel access scheme based on the sensing outcome. In the absence of any PU on a typical channel, SUs transmit within such a channel following the overlay spectrum access scheme and switch to the underlay spectrum access scheme (with limited transmission interruption experience) when at least one PU arrives on such a channel. The hybrid scheme is capable of improving SUs' throughput, while also ensuring that the QoS of PUs is satisfied [4]. Under this spectrum access scheme, SUs transmit with a higher data rate in the absence of PUs and do not vacate the channel whenever a PU arrives unlike in the conventional overlay channel access model, but adopt power control techniques by switching to underlay channel access scheme using the mode switching rate parameter. Hence hybrid spectrum access model can improve SUs' channel usage experience [5].

1.2. Age of Information

Age of information (AoI) [6] is a new metric that has recently been attracting a lot of attention owing to the need to characterize the freshness (or timeliness) of packets (or data) at the receiving nodes. With AoI, the freshness of packets sent by the transmitting nodes can be determined at their respective intending nodes. Such a parameter is very useful, especially when the timeliness of data at the receivers is important for efficient system performance. While the delay metric can only reflect timeliness of a packet at the time instants at which the packet is successfully decoded at the intending receiver, AoI allows an opportunity to measure the timeliness of a packet at the intending receiving node at any given time instant [7]. This implies that the timeliness of the received packet is measured from the receiving node's perspective when the AoI is used [8].

In [7], the analysis for the average peak AoI was derived in a cognitive radio-based internet of thing (IoT) systems with a single primary IoT system and single secondary IoT system. Similarly, the authors in [8] studied the average AoI of energy harvesting SU nodes in a multiuser CRN, while the analysis for the average AoI in the primary node was obtained for a single primary transmitter-receiver pair in [9]. The spatial distribution

of the mean peak AoI was characterized in [10] using the tool of stochastic geometry (SG). The SG is a very useful approach that provides efficient mathematical and statistical mechanisms useful in the study and analyses of random spatial patterns. Such random spatial patterns, known as point processes—defined as set of locations that are distributed within a certain designated region—are normally generated using stochastic mechanisms and are known to be important elements of SG. With the use of random point patterns, the distribution of users in CRN can be realistically captured, while the analysis resulting from such a process can be accurate and tractable, albeit under various simplifications and assumptions [2,11]. The effectiveness of SG in obtaining various tractable analytical solutions has been demonstrated in different works. Interested readers are referred to [12–14] for more details.

Finally, the analysis for the throughput as well as the average AoI was obtained for cellular-based IoT networks in [15], while the analysis for the AoI in a static Poisson network was also obtained in [16]. As will be seen in the remaining sections of this paper, the analysis for the AoI depends on the transmission and success probabilities in the network. We adopt the tool of SG in order to obtain the analysis for this success probability and captured the aggregate interference within the considered cognitive network in the analysis.

1.3. Related Works

The hybrid channel access model was first proposed in [1] and has since been adopted in the domain of CRN. A hybrid channel access model for classified SUs with channel bonding mechanism was presented in [3] for CRN, while the hybrid spectrum sharing scheme-based power allocation methods for SUs' data rate maximization under PUs' QoS constraints was investigated by Zou et al. [4]. When transmitting under the overlay channel access scheme, power is allocated to any SU in proportion to its payment without additional constraints by the relay, hence, achieving a higher data rate and throughput. Under the underlay channel access scheme, however, relay assigns power to SUs based on PUs' QoS constraints. The analyses for the hybrid spectrum access model were provided in [1,5,17,18].

Similarly, a hybrid mode strategy for dynamic spectrum access using double threshold energy detection and Markov model was considered in [19], while a hybrid mode-based resource allocation method was proposed in [20], where the secondary base station allocates sub-channels and total power to SUs based on the received channel state information. In a similar work, the achievable throughput was maximized by [21]. Bhowmick et al. [22] proposed the hybrid and modified hybrid modes-based CRN schemes with the aim of improving throughput while reducing outage probability. A modified hybrid model was defined as one in which SU transmits in both sensing and detection cycles. The switching rate also known as the hybrid rate was optimized in [5] by maximizing SUs' throughput while satisfying PUs' QoS constraints. The analysis for departure rate [1,17], outage probability [1,4,17,18,23], bit error rate [18] and achievable rate [4] were subsequently obtained.

While most of the preliminary works considered the relationship between the underlay and overlay modes in hybrid spectrum access mode, most of the analysis presented in such works did not capture the mutual interference that can result due to the transmissions of multiple PUs, SUs as well as sensing error. This was considered in the analyses presented in [1,5,17,18]. However, these analyses did not capture the spatial distribution of users—an essential requirement to obtain accurate analysis when modeling interference in wireless networks, while intra-network and inter-network interference were largely ignored. These spatial distributions are well captured in this paper through the use of point process—an important element of SG. We investigate users' performance in the hybrid mode-based CRN, while capturing intra-network and inter-network interference in the analysis. We obtained tractable analyses for the success probability, network throughput and average AoI for the hybrid CRN and compared the network performance under the hybrid mode with the conventional overlay and underlay modes.

1.4. Contributions and Organisation

The contributions of this paper are thus summarized as follow:

- By capturing the spatial distributions of users in both primary and secondary networks following two independent Poisson point processes (PPPs), we obtained tractable analysis for the conventional success probability (i.e., service/update delivery rate) in the considered hybrid spectrum access CRN. Since success probability is a location-dependent random variable, the analysis for the distribution of conditional success probability known as Meta distribution was further obtained.
- Using the analysis of the conventional success probability obtained, we derived expressions for the network throughput in the hybrid spectrum access CRN for both primary and secondary networks.
- Finally, based on the analysis of the conditional success probability, the expression for conditional average AoI was presented for the underlay, overlay and hybrid spectrum access CRN. To the best of our knowledge, this is the first work that investigates AoI in the hybrid spectrum access-based CRN.

In the remainder of this paper, we present the network model in Section 2, while the details of the analysis for the success probability are presented in Section 3. Section 4 presents the analysis of the network throughput and the conditional average AoI, while Section 5 presents the results of the numerical simulations. Finally, Section 6 concludes the paper.

2. Network Model

We considered a massive CRN as a network with multiple primary and secondary transmitter-receiver pairs within the Euclidean space as shown in Figure 1, where primary transmitters (PTs) and secondary transmitters (STs) are distributed following two independent homogeneous PPPs (HPPPs) Φ_p and Φ_s of intensities λ_p and λ_s respectively. The term massive or large-scale CRN is often used when multiple PUs and SUs are transmitting within the same channel. In such a network, intra-network and inter-network interference can influence the performance of the network and must be captured in the network modeling. A typical primary connection is made up of a PT $x_k^p \in \Phi_p$ and a primary receiver (PR) y_k^p , while any typical secondary connection is made up of an ST $x_k^s \in \Phi_s$ and a secondary receiver (SR) y_k^s . In order to meet the channel access demands in secondary networks, STs are permitted to transmit to their respective receivers at any period of time following the hybrid spectrum access technique.

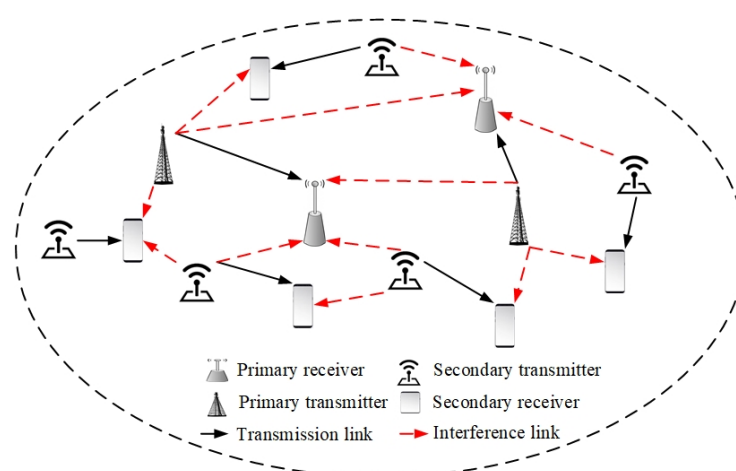


Figure 1. Users' distribution in massive CRN.

Since PUs' deployments are rather planned in real-life deployments, we assumed that each PT is at least a distance D from its nearest PT to ensure minimum repulsion between PU transmitters that are normally observed in real-life deployments. Although

PTs' distribution may not actually follow PPP in practical systems, existing efforts [2,24] showed that the PPP can provide an accurate approximation for the distribution of PTs. Each PT has a dedicated PR, whose location is at a distance r_p in a random orientation. Similarly, each ST has a dedicated SR, whose location is at a distance r_s in a random orientation. Based on the displacement theorem [25], the locations of PRs and SRs are also known to follow independent HPPPs of intensities λ_p and λ_s respectively. It was further assumed that each transmitter is connected to its nearest receiver [26].

We considered a discrete, time-slotted system, in which STs are required to perform channel sensing at the beginning of each time slot in order to detect the state of PTs within such channels, before generating packets for their respective receivers. We assumed that packet generation occurs right before transmission and that the transmission of one packet occupies a one-time slot. Any ST transmits in the underlay mode with an appropriate power control technique with transmit power $P_s = P_s^U$ if the sensing outcome reveals the presence of at least one active PT on the channel and transmits in the overlay mode with a higher rate (i.e., ST full transmit power, $P_s = P_s^O$) if otherwise. At the detection of the presence or absence of primary signal, ST switches between underlay and overlay modes in order to maximize its throughput, while ensuring that PTs' QoS constraint is satisfied. Since SUs are expected to be energy-efficient devices, continuous channel sensing can degrade the efficiency of each SU. Hence, channel sensing may be carried out by some randomly dedicated SUs at each time slot. The outcome of the channel sensing can then be made available to all SUs via a dedicated error-free link.

STs' transmissions are allowed in the underlay mode at any time slot as long as the interference received at any PR within such location is below the pre-defined interference temperature. Hence, the transmit power of any typical ST in the underlay mode (i.e., P_s^U) is subject to power control technique and can be obtained as [1]

$$P_s^U = \begin{cases} P_s^{\max}, & \text{if } h_{sp}||sp||^{-\alpha} \leq \frac{I_d}{P_s^{\max}} \\ \frac{I_d}{h_{sp}||sp||^{-\alpha}}, & \text{if } h_{sp}||sp||^{-\alpha} > \frac{I_d}{P_s^{\max}}, \end{cases} \quad (1)$$

where P_s^{\max} is the maximum transmit power of any ST in the underlay mode, I_d is the maximum permissible interference level at any PU, h_{sp} represents the independent and identically distributed exponential fading coefficient between any ST and the tagged PR, $||sp||$ is the Euclidean distance between any ST and PR and represents the large-scale path loss attenuation between such ST and PR, and α is the path loss exponent. For any typical PR y_k^p located at a distance r_p from its paired PT x_k^p assumed to be located at the origin of its coverage region [2,24], the signal to interference plus noise ratio (SINR) received at y_k^p in time slot t is given as

$$SINR_{y_k^p,t} = \frac{P_p h_{x_k^p,y_k^p} r_p^{-\alpha}}{\sigma^2 + I_{pp} + I_{sp}}, \quad (2)$$

where P_p is the fixed transmission power of PT, h_{ab} is the exponentially distributed channel fading from transmitter a to receiver b , I_{pp} is the interference from active PTs except x_k^p at the y_k^p , I_{sp} is the interference from active STs at the y_k^p and σ^2 is an independent Gaussian thermal noise signal power. Similarly, for any typical SR y_k^s located at a distance r_s from its paired ST x_k^s , the SINR received at y_k^s is given as

$$SINR_{y_k^s,t} = \frac{P_s h_{x_k^s,y_k^s} r_s^{-\alpha}}{\sigma^2 + I_{ss} + I_{ps}}, \quad (3)$$

where I_{ss} is the interference from active STs except x_k^s at the y_k^s and I_{ps} is the interference from active PTs at the y_k^s . Next, we obtained the analyses for the success probability and conditional success probability in both primary and secondary networks following the network description provided in this section.

3. Analysis of Success Probability

We considered a typical system, where each transmitting node generates and sends packets to its intending receiver following an independent and identically distributed Bernoulli process $v_{Tr,t} \in [0, 1]$ in each time slot t , where $Tr = p$ for PT and $Tr = s$ for ST. Since we considered a discrete-time system, where packet generations at various nodes are independent, as in the conventional CRN, packet generation at each node can be modeled as a Bernoulli process. This implies that any packet is transmitted the same time slot it was generated. A failed transmission is repeated in a future time slot until it is successful. A transaction is successful if the received SINR at the intending receiver is greater than the predefined SINR θ_{Tr} threshold. A successfully received packet is removed from the channel. We assumed that each receiver is able to generate an ACK (for successful transmission) or NACK (for failed transmission) through a dedicated error-free channel in a negligible time instant to inform its paired transmitter on the status of its transmission.

Assumption 1. *The realization of the network was considered to be static, i.e., the locations of all transmitting and receiving nodes remain constant in all time slots. Hence, the transmission success probability obtained in each time slot is independent of other slots. We henceforth drop the notation t .*

Remark 1. *This commonly adopted assumption is necessary to simplify the time-domain evolution and to avoid complicated analysis. The same assumption is made in [16,27,28], etc.*

3.1. Success Probability in Hybrid Cognitive Networks

The success probability is given as the average delivery rate (or service completion rate) at any test receiver. Under the hybrid spectrum access mode, such an analysis depends on the transmissions in both the overlay and underlay modes.

3.1.1. Analysis in the Primary Network

Considering a typical (i.e., any arbitrarily selected) primary transmitter-receiver pair in the hybrid CRN, the success probability can be obtained as

$$\mu_p^h = (1 - p_m)[\varepsilon(1 - P_{o,p}^U) + (1 - \varepsilon)(1 - P_{o,p}^O)] + p_m(1 - P_{o,p}^{OI}), \tag{4}$$

where p_m is the probability of misdetection of PT signal by ST and ε is the ST switching rate between underlay and overlay modes. The switching rate $\varepsilon = 0$ indicates a fully or conventional overlay mode, $\varepsilon = 1$ indicates a fully underlay mode, while $0 < \varepsilon < 1$ indicates the hybrid model. Similarly, $P_{o,p}^U$ is the PU outage probability as in the conventional underlay mode, $P_{o,p}^O$ is the PU outage probability as in the conventional overlay mode and $P_{o,p}^{OI}$ is the PU outage probability when there is a misdetection of PU signal. Generally, the success probability at a receiving node is equivalent to $\mu = 1 - P_{outage}$, where P_{outage} is the outage probability at such a receiving node. The outage probability at any typical PR y_k^p is obtained from (2) as [2]:

$$P_{outage} = P(SINR_{y_k^p} \leq \theta_p) = 1 - \exp(-s\sigma^2)\mathcal{L}_{I_{pp}}(s)\mathcal{L}_{I_{sp}}(s), \tag{5}$$

where \mathcal{L}_I is the Laplace transform of aggregate interference I taken at $s = \frac{\theta_p r_p^\alpha}{P_p}$. The parameter $\theta_p = 2^{\tau-1}$, where τ is the data rate for primary transmission. From (4), it is clear that we must first obtain the analysis for the conventional underlay and overlay transmissions before the analysis for the hybrid transmission can be obtained.

1. Underlay model: In the presence of at least one PT, STs coexist with active PTs as in the underlay mode, provided that its location is not within the exclusion region D of any active PT. Hence the PU outage probability at any typical PR y_k^p is obtained from (5) as

$$P_{o,p}^U(y_k^p) = 1 - \exp(-s\sigma^2)\mathcal{L}_{I_{pp}}(s)\mathcal{L}_{I_{sp}}(s).$$

In a simplified CRN, only a single PT x_k^p transmits on any channel, thus $\mathcal{L}_{I_{pp}} = 1$. However, in a massive or large scale CRN considered in this paper, multiple PTs can co-exist within the same channel, hence $I_{pp} = \sum_{x_i^p \in \Phi_p \setminus x_k^p} P_p h_{x_i^p y_k^p} \|x_i^p y_k^p\|^{-\alpha}$ [2]. $\mathcal{L}_{I_{pp}}$ is expressed as

$$\mathcal{L}_{I_{pp}}(s) = E \left\{ \exp \left(-s \sum_{x_i^p \in \Phi_p \setminus x_k^p} P_p h_{x_i^p y_k^p} \|x_i^p y_k^p\|^{-\alpha} \right) \right\}, \tag{6}$$

where $\|ab\|$ is the large-scale path loss attenuation between the transmitter a and receiver b . Under Rayleigh fading assumption, h_{ab} is assumed to be independent and identically distributed exponential random variables with unit mean, i.e., $h_{ab} \sim \exp(1)$. By applying the probability generating function of PPP to (6),

$$\mathcal{L}_{I_{pp}}(s) = \mathcal{L}(\lambda_p^I, P_p, s) = \exp \left\{ -\lambda_p^I v_p \frac{\pi^2 \delta}{\sin(\pi \delta)} P_p^\delta s^\delta \right\}, \tag{7}$$

where $\delta = \frac{2}{\alpha}$ and $\lambda_p^I = \lambda_p P_a$. The expression of P_a can be obtained through the void probability technique, $P_a = \exp(-\lambda_p \pi D^2)$, which captures the repulsion between active PTs. The resulting point process can as well be approximated as a PPP Φ_p^I of intensity λ_p^I . The derivation of (7) is straightforward from [29]. Similarly,

$$\mathcal{L}_{I_{sp}}(s) = \mathcal{L}(\lambda_s^I, P_s^U, s),$$

where $\lambda_s^I = \lambda_s P_b$, knowing that an ST will only transmit when its location is outside the region of radius D of any active PTs. Hence, $P_b = \exp(-\lambda_p^I \pi D^2)$. The resulting point process in this case is better represented as hole processes. However, to avoid unnecessary complicated analysis, we approximated the distribution of active STs as independent PPP of equidense intensity λ_s^I .

2. Overlay model: In the absence of active STs, PTs transmit in the overlay mode. Hence the interference from STs is normally assumed to be zero in the overlay mode provided that there is no inter-channel interference. With this, $\mathcal{L}_{I_{sp}} = 1$ and

$$P_{o,p}^O(y_k^p) = 1 - \exp(-s\sigma^2) \mathcal{L}(\lambda_p^I, P_p, s). \tag{8}$$

Finally, when there is misdetection of PTs signal by SUs, active STs transmit with full transmit power $P_s^O > P_s^U$ thereby causing more interference in the primary network. Hence, at any typical PR,

$$\mathcal{L}_{I_{sp}}(s) = \mathcal{L}(\lambda_s^I, P_s^O, s),$$

$$P_{o,p}^{OI}(y_k^p) = 1 - \exp(-s\sigma^2) \mathcal{L}(\lambda_p^I, P_p, s) \mathcal{L}(\lambda_s^I, P_s^O, s). \tag{9}$$

3.1.2. Analysis of the Secondary Network

The success probability at any test SR under the hybrid spectrum access mode can be obtained at any given switching rate ε as

$$\mu_s^h = p_q(1 - p_f)(1 - P_{o,s}^O) + (1 - p_q)p_m(1 - P_{o,s}^{OI}) + (1 - \rho)\varepsilon[p_q p_f(1 - P_{o,s}^U) + (1 - p_q)(1 - p_m)(1 - P_{o,s}^{UI})], \tag{10}$$

where $P_{o,s}^O$ is the SU outage probability as in the conventional overlay mode provided there was no misdetection, $P_{o,s}^{UI}$ is the SU outage probability as in the underlay mode with a false alarm (at least from PU's perspective), $P_{o,s}^{OI}$ is the SU outage probability in overlay mode when there was misdetection, $P_{o,s}^U$ is the SU outage probability in the underlay mode with interference from PTs, p_f is the probability of false alarm, p_q is the probability that there is no PT in the channel and ρ represents the penalty term due to periodic monitoring of the interference channel in underlay mode.

The outage probability at any typical SR y_k^s is obtained from (3) as

$$P_{outage} = P(SINR_{y_k^s} \leq \theta_s) = 1 - \exp(-z\sigma^2)\mathcal{L}_{I_{ss}}(z)\mathcal{L}_{I_{ps}}(z), \tag{11}$$

where $z = \frac{\theta_s r_s^\alpha}{P_s}$. Similarly, the parameter $\theta_s = 2^\eta - 1$, where η is known as the data rate for secondary transmission.

1. Underlay model: In the presence of at least one PT, STs coexist with active PTs as in the conventional underlay mode, hence the SU's outage probability at any typical SR y_k^s at $z = \frac{\theta_s r_s^\alpha}{P_s^U}$ is given as

$$P_{o,s}^{UI}(y_k^s) = 1 - \exp(-z\sigma^2)\mathcal{L}_{I_{ss}}(z)\mathcal{L}_{I_{ps}}(z). \tag{12}$$

Similar to (7), we also know that

$$\mathcal{L}_{I_{ss}}(z) = \mathcal{L}(\lambda_s^I, P_s^U, z),$$

$$\mathcal{L}_{I_{ps}}(z) = \mathcal{L}(\lambda_p^I, P_p, z).$$

Finally, when STs transmit in the underlay mode as a result of a false alarm, the only interference generated is from other active STs, hence,

$$P_{o,p}^U(y_k^s) = 1 - \exp(-z\sigma^2)\mathcal{L}(\lambda_s^I, P_s^U, z). \tag{13}$$

2. Overlay mode: In overlay mode, the interference from PTs can be assumed to be zero when there is no active PT on the channel. With this, $\mathcal{L}_{I_{ps}} = 1$ and

$$P_{o,s}^O(y_k^s) = 1 - \exp(-z\sigma^2)\mathcal{L}(\lambda_s^I, P_s^O, sz = \frac{\theta_s r_s^\alpha}{P_s^O}). \tag{14}$$

When there is misdetection of PTs signal, STs transmit with full transmit power $P_s^O > P_s^U$ thereby generating higher interference at any active PR, while also receiving interference from active PTs. Hence, at any typical SR,

$$\mathcal{L}_{I_{ps}}(sz) = \mathcal{L}(\lambda_p^I, P_p, sz),$$

$$P_{o,s}^{OI}(y_k^s) = 1 - \exp(-sz\sigma^2)\mathcal{L}(\lambda_s^I, P_s^O, sz)\mathcal{L}(\lambda_p^I, P_p, sz). \tag{15}$$

3.2. Conditional Success Probability

The analysis obtained in Section 3.1 is not sufficient when characterizing non-linear metrics such as the average AoI in any wireless network since the probability of successful transmission is a location-dependent random variable, hence the need to obtain the meta distribution [30], i.e., the distribution of the conditional transmission success probability.

3.2.1. Conditional Success Probability in Primary Network

The conditional success probability at any typical PR y_k^p (expressed as $\mu_{y_k^p}^I$) is thus given as

$$\mu_{y_k^p}^I = P(SINR_{y_k^p} > \theta_p | \Phi, \forall \Phi = \Phi_p^I \cup \Phi_s^I). \tag{16}$$

Lemma 1. *In the conventional underlay mode, the conditional success probability $\mu_{y_k^p}^{IU}$ can be expressed as*

$$\mu_{y_k^p}^{IU} = \exp\left(\frac{\theta_p r_p^\alpha \sigma^2}{P_p}\right) \prod_{x_i^p \in \Phi_p^I \setminus x_k^p} \left(\frac{v_p}{1 + \theta_p r_p^\alpha \|x_i^p\|^{-\alpha}} + 1 - v_p \right) \prod_{x_i^s \in \Phi_s^I} \left(\frac{v_s}{1 + \theta_p r_p^\alpha \|x_i^s\|^{-\alpha} \frac{P_s^U}{P_s}} + 1 - v_s \right). \tag{17}$$

Proof. By substituting (2) into (16), the analysis for the success probability can be obtained conditioned on Φ . The proof is straightforward from Appendix A of [20]. \square

However, the analysis in (17) is difficult to solve, hence its b-th moment as $\sigma^2 \rightarrow 0$ is obtained as

$$M_b = E_{y_k^p}[(\mu_{y_k^p}^{IU})^b] = E_{r_p} \left[E \prod_{x_i^p \in \Phi_p^I \setminus x_k^p} \left(1 - \frac{E[v_p|\Phi]}{1 + \frac{\|x_i^p\|^\alpha}{\theta_p r_p^\alpha}} \right)^b E \prod_{x_i^s \in \Phi_s^I} \left(1 - \frac{E[v_s|\Phi]}{1 + \frac{\|x_i^s\|^\alpha P_p}{\theta_p r_p^\alpha P_s^U}} \right)^b \right]. \quad (18)$$

Following the analysis in [28,30], the b-th moment of $\mu_{y_k^p}^{IU}$ can be expressed as

$$M_b = \exp \left\{ -\lambda_p \theta_p^\delta r_p^2 \frac{\pi^2 \delta}{\sin(\pi \delta)} \sum_{k=1}^\infty \binom{b}{k} \binom{\delta-1}{k-1} v_p^k \right\} \exp \left\{ -\lambda_s \left(\frac{\theta_p P_s^U}{P_p} \right)^\delta r_p^2 \frac{\pi^2 \delta}{\sin(\pi \delta)} \sum_{k=1}^\infty \binom{b}{k} \binom{\delta-1}{k-1} v_s^k \right\}. \quad (19)$$

The meta distribution can be approximated following the approach presented in [30,31] with the beta distribution as

$$P[\mu_{y_k^p}^{IU} \leq x] = I_x(\beta_1, \beta_2),$$

where the parameter $I_x(\cdot, \cdot)$ is known as the regularized incomplete beta function and

$$\beta_1 = \frac{M_1(M_1 - M_2)}{M_2 - M_1^2},$$

$$\beta_2 = \frac{(M_1 - M_2)(1 - M_1)}{M_2 - M_1^2}.$$

M_1 and M_2 are the first and second moment of $\mu_{y_k^p}^{IU}$ given in (19).

Lemma 2. The conditional success probability at any typical PR y_k^p in the conventional overlay mode is given as

$$\mu_{y_k^p}^{IO} = \exp\left(\frac{\theta_p r_p^\alpha \sigma^2}{P_p}\right) \prod_{x_i^p \in \Phi_p^I \setminus x_k^p} \left(\frac{v_p}{1 + \theta_p r_p^\alpha \|x_i^p\|^{-\alpha}} + 1 - v_p \right).$$

Its b-th moment as $\sigma^2 \rightarrow 0$ is obtained as

$$M_{b,overlay} = \exp \left\{ -\lambda_p \theta_p^\delta r_p^2 \frac{\pi^2 \delta}{\sin(\pi \delta)} \sum_{k=1}^\infty \binom{b}{k} \binom{\delta-1}{k-1} v_p^k \right\}. \quad (20)$$

Proof. Under the conventional overlay CRN, the interference from STs is neglected. Hence, the conditional success probability depends only on the interference from other active PTs as in Section 3.1. Finally, the case of misdetection is straightforward from (19) by taking $P_s = P_s^O$, while the analysis for the hybrid case is straightforward from (4). \square

3.2.2. Conditional Success Probability in Secondary Network

Similar to the case of the primary network, the conditional success probability at any typical SR y_k^s is given as

$$\mu_{y_k^s}^I = P(SINR_{y_k^s} > \theta_s | \Phi, \forall \Phi = \Phi_p^I \cup \Phi_s^I). \quad (21)$$

In the conventional underlay mode, the conditional success probability as $\sigma^2 \rightarrow 0$ is obtained as

$$\mu_{y_k^s}^{IU} = \prod_{x_i^s \in \Phi_s^I \setminus x_k^s} \left(\frac{v_s}{1 + \theta_s r_s^\alpha \|x_i^s\|^{-\alpha}} + 1 - v_s \right) \prod_{x_i^p \in \Phi_p^I} \left(\frac{v_p}{1 + \theta_s r_s^\alpha \|x_i^p\|^{-\alpha} \frac{P_p}{P_s^U}} + 1 - v_p \right). \quad (22)$$

Its b-th moment is similarly obtained as

$$M_b = E_{y_k^s} [(\mu_{y_k^s}^{IU})^b] = E_{r_s} \left[E \prod_{x_i^s \in \Phi_s^I \setminus x_k^s} \left(1 - \frac{E[v_s|\Phi]}{1 + \frac{\|x_i^s\|^\alpha}{\theta_s r_s^\alpha}} \right)^b E \prod_{x_i^p \in \Phi_p^I} \left(1 - \frac{E[v_p|\Phi]}{1 + \frac{\|x_i^p\|^\alpha}{\theta_s r_s^\alpha} \frac{P_p}{P_s^U}} \right)^b \right]. \quad (23)$$

From (23), the approximation for the conditional success probability in the secondary network can as well be obtained for the conventional underlay, conventional overlay and the case of misdetection. The analysis for the hybrid is then straightforward from (10).

4. Analysis for Network Throughput and Average Age of Information

Based on the analyses presented in Section 3, we now further provide analyses for the network throughput and the AoI. The analysis for network throughput follows from Section 3.1, while the analysis for the AoI follows from Section 3.2.

4.1. Network Throughput

In any given network, the throughput can be defined as the mean number of packets (i.e., information) that were successfully received at the intending receivers within the considered area at any unit time [15]. The average network throughput in the primary network (represented as T_N^p) can be obtained as

$$T_N^p = \lambda_p^I v_p \log_2(1 + \theta_p) \mu_{y_k^p}. \quad (24)$$

Similarly, the network throughput in the secondary network can be derived as

$$T_N^s = \lambda_s^I v_s \log_2(1 + \theta_s) \mu_{y_k^s}. \quad (25)$$

By substituting the analyses in Section 3.1 into (24) and (25), the network throughput for the overlay, underlay and hybrid CRNs can be obtained. This will be compared in Section 5.

4.2. Average Age of Information

The AoI is an important metric in any wireless communications network as it defines the freshness of data intended for a typical receiving node from the receiver’s perspective. Note that timeliness is necessary to obtain a reliable system since a packet that arrives late may fail to achieve its intending purpose. At any given time stamp t (that is, observation time), the AoI $\Delta(t)$ is the difference between the current observation point t and the time at which the packet was generated $G(t)$ [32], i.e.,

$$\Delta(t) = t - G(t). \quad (26)$$

The evolution of the AoI can be formalized as

$$\Delta(t+1) = \begin{cases} \Delta(t) + 1, & \text{transmission failure} \\ t + 1 - G(t), & \text{otherwise.} \end{cases} \quad (27)$$

This metric captures the sum of packet waiting time in the queue, as well as the time spent in service and can be represented as shown in Figure 2. Given that X_k is the number of slots between the successful delivery of any two consecutive k -th and $(k + 1)$ -th packets, while Y_k depicts the sum of AoI, X_k is given as

$$X_k = \sum_{i=1}^M I_i, \tag{28}$$

where M is a random variable that depicts the number of attempted transmissions between two successfully received packets. Similarly,

$$Y_k = \sum_{k=t_k}^{t_{k+1}} \Delta(k). \tag{29}$$

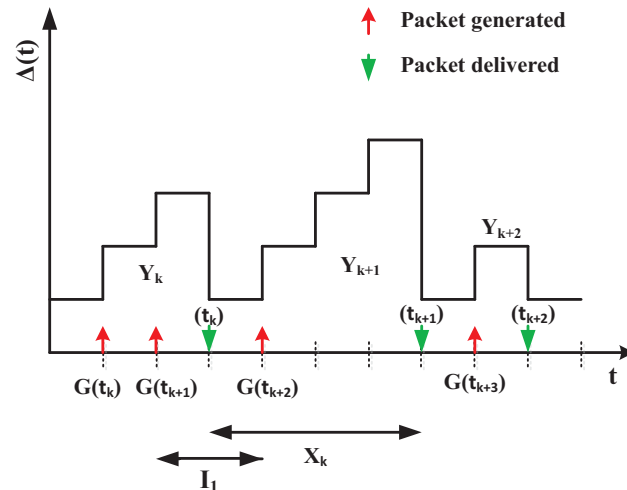


Figure 2. Evolution of AoI. I_i denotes the inter-arrival time slots, X_k is the number of slots between successful delivery of two consecutive packets and Y_k is the sum of AoI between t_k and t_{k+1} .

From [15,33], we know that the analysis for the average AoI can be obtained for any period of W slots where there is an L number of successfully delivered (i.e., decoded) packets. This average AoI is given as

$$\Delta(W) = \frac{1}{W} \sum_{k=1}^W \Delta(k) = \frac{1}{W} \sum_{k=1}^L Y_k = \frac{L}{W} \frac{1}{L} \sum_{k=1}^L Y_k. \tag{30}$$

Taking $\lim_{W \rightarrow \infty} \frac{L}{W} = \frac{1}{E[X]}$ with $\lim_{L \rightarrow \infty} \frac{1}{L} \sum_{k=1}^L Y_k = E[Y]$,

$$\Delta = \lim_{W \rightarrow \infty} \Delta(W) = \frac{E[Y]}{E[X]}.$$

A careful observation of Figure 2 shows that, Y_k can be obtained as

$$Y_k = \sum_{m=1}^{X_k} m = \frac{X_k^2}{2} + \frac{X_k}{2}.$$

From (30),

$$\Delta = \frac{E[X^2]}{2E[X]} + \frac{1}{2}. \tag{31}$$

It is worth noting that the distribution of X_k in (31) as given in (28) depends on the arrival rate v_{Tr} (i.e., probability of transmission) and the probability of successful transmission μ_y^1 . Hence the distribution of X_k is a random process. It becomes immediately clear that the average AoI observed at any tagged receiver depends on the spatial distributions of users, thus the need to obtain the analysis for the conditional average AoI as given in the following Lemma.

Lemma 3. The conditional average AoI obtained at a tagged receiver y_k^{Tr} given that $\Phi = \Phi_p^I \cup \Phi_s^I$ can be obtained as

$$\Delta(y_k^{Tr} | \Phi = \Phi_p^I \cup \Phi_s^I) = \frac{1}{v_{Tr} \mu_{y_k^{Tr}}^I}. \quad (32)$$

Proof. The proof is straightforward from [15,33] and is omitted for brevity. From (32), the average AoI observed by any test PR and SR for each mode can be obtained based on the analysis in Section 3.2. \square

5. Numerical Results and Simulation

We now provide some details and outcomes of numerical simulations carried out in order to demonstrate the performance of both PUs and SUs under the proposed approach. The delivery rate—the success probability for any test transmitter—is determined as the probability that its intending paired receiver does not experience outage as a result of other users' activities at any observation period. We compared the performance of the hybrid spectrum access scheme with conventional overlay and underlay spectrum access schemes. This is necessary to demonstrate the advantages of the hybrid spectrum access model over the widely studied conventional overlay and underlay spectrum access models. We further carried out the Monte Carlo simulation averaged over 50,000 channel realizations in order to validate the presented analytical approach. Except otherwise stated, the parameters used for simulation are presented in Table 1.

Table 1. Simulation parameters.

Parameter	Definition	Value
λ_s	Distribution of secondary transmitter-receiver pairs	0.3
λ_p	Distribution of primary transmitter-receiver pairs	0.03
r_p	Distance between any tagged primary transmitter-receiver pair	0.5 m
r_s	Distance between any tagged secondary transmitter-receiver	0.1 m
P_p	PT's transmission power signal	0 dB
P_s^O	ST's transmission power signal in the overlay mode	−32 dB
P_s^U	ST's transmission power signal in the underlay mode	−36 dB
α	Path-loss exponent	4
D	Coverage region of any PT	1.2 m

In order to ensure that the PUs' QoS constraints are satisfied, it is important to guarantee a high packet delivery rate at PRs. PUs service delivery rate can however be degraded by the activities of SUs when channel sensing is not well coordinated. As shown in Figure 3, an increase in switching rate reduces the PU service completion rate (i.e., the delivery rate) owing to more activities of SUs in the underlay mode, while an increase in the probability of misdetection significantly affects the services of active PUs since STs transmit with full transmit power in the presence of PUs. It is hence important to ensure that channel sensing is well-coordinated among SUs to improve PUs detections.

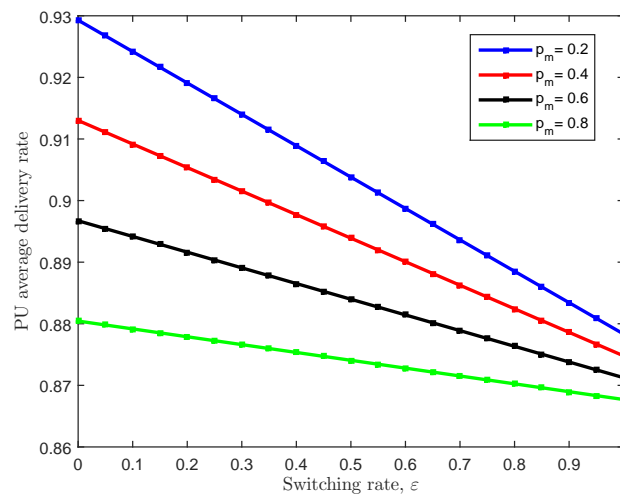


Figure 3. Conventional service completion rate in the primary network under hybrid mode ($\theta_p = 9.5$ dB, $v_p = v_s = 1$).

Intuitively, the outage probability (PUs and SUs) should increase with an increase in the SINR threshold θ_{Tr} , a parameter that is proportional to the data transmission rate. As expected, an increase in the required data rate of the primary link increases the outage probability in the primary network. This shows that the PU service delivery rate will reduce with an increase in data rate irrespective of the spectrum access mode. As presented in Figure 4, when $\epsilon = 0.25$ and $p_m = 0.2$, the transmission under the overlay spectrum access scheme produces a lower chance of outage than the transmission under the hybrid spectrum access scheme. This is expected since interference in the conventional large-scale overlay scheme is dominated by interference from active PTs only. Transmissions in the conventional overlay scheme, however, means low throughput for secondary transmissions, making the hybrid scheme a more preferred spectrum access model from SUs’ perspective.

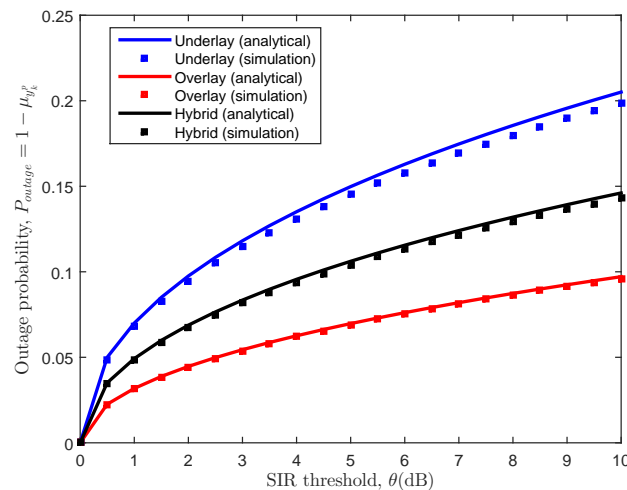


Figure 4. Outage probability with an increase in transmission data rate ($v_p = v_s = 1$).

The effect of the required data rate on the success probability in the secondary network is presented in Figure 5. While an increase in the required data rate can reduce the success probability, accessing a channel under the hybrid scheme is shown to improve the overall success probability in secondary networks owing to the fact that, SUs are able to access channel for transmissions at any time. Also, SUs can transmit with full transmit power in the absent of PUs and can switch to the underlay spectrum access scheme when at least one PU is present. Hence, SUs’ success probability can be improved under the hybrid spectrum access scheme. The rate of PUs’ transmission can also affect SUs’ success probability in

both the overlay and underlay models as shown in Figure 5. On channels with a more dominant presence of PUs, SUs do not get enough access to transmit, hence the reason for lower delivery rate in such a scenario.

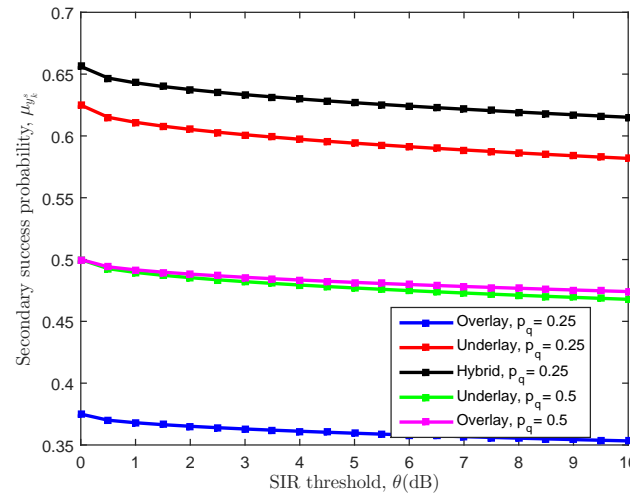


Figure 5. Average delivery rate in the secondary network, ($p_f = 0.25, \epsilon = 0.5, \rho = 0.2\epsilon, p_m = 0.25, v_p = v_s = 1$).

With an improved detection of PU signal, the QoS constraints of PUs can be met, while the average delivery rate of SUs reduces owing to the transmission constraints when at least one PU is present on the channel. The hybrid spectrum access model shows improved performance over the overlay mode and can continue to produce a remarkable higher average delivery rate for secondary transmissions even when $p_d = 1$ as shown in Figure 6.

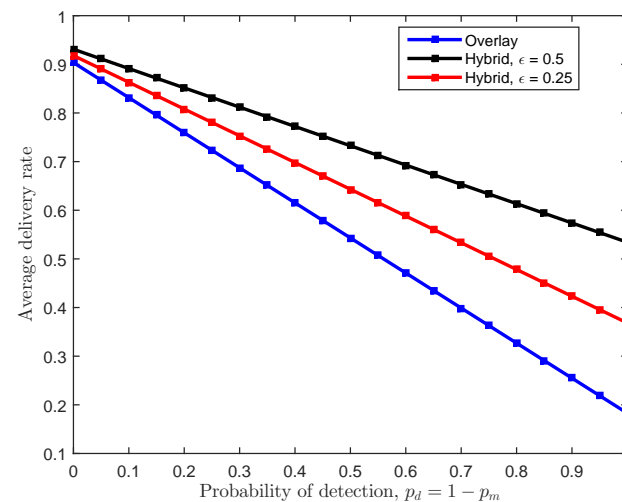


Figure 6. Effect of PU signal detection probability on SU delivery rate, ($p_q = 0.25, p_f = 0.25, \rho = 0.2\epsilon, v_p = v_s = 1$).

As expected, the network throughput in the primary network, as presented in Figure 7 under the selected simulation parameters decreases with an increase in the distance between the tagged primary transmitter-receiver pair since the transmit power of PT is fixed, while the effect of interference can also influence the network performance, especially in the underlay and hybrid modes. Similar relationships were observed in the secondary network as shown in Figure 8. Furthermore, lower network throughput is observed in the overlay mode for SUs as shown in Figure 8 since SUs have limited access to transmit. As expected, SUs benefit more when transmitting under the hybrid spectrum access mode.

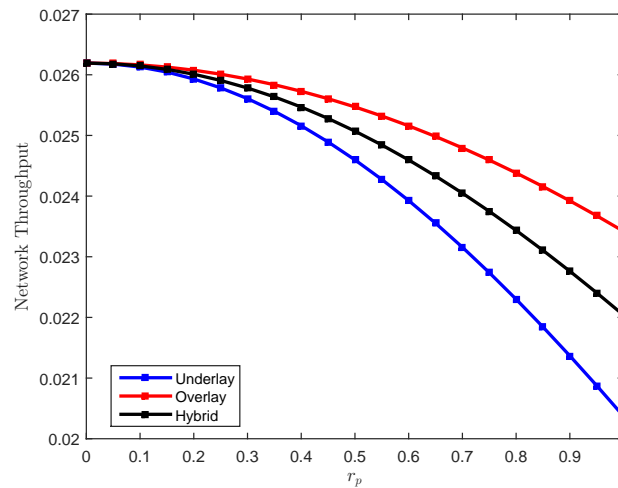


Figure 7. Network throughput in the primary network, ($\theta_p = 9.5$ dB, $v_p = v_s = 0.5$).

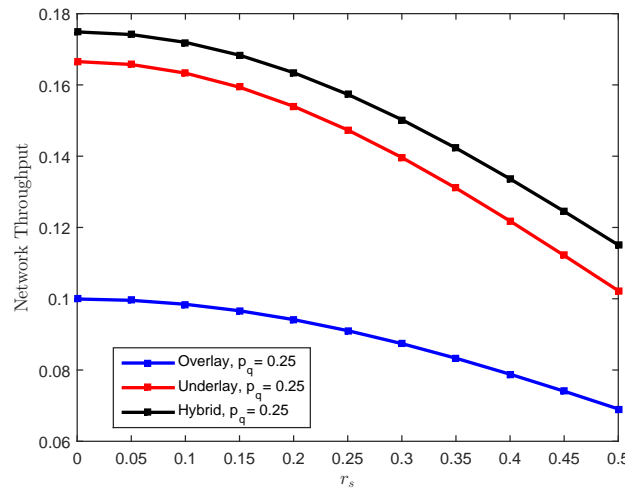


Figure 8. Network throughput in the secondary network, ($\theta_s = 9.5$ dB, $v_p = v_s = 0.5$).

As previously mentioned, the analysis of the conditional average AoI depends on the conditional success probability—a parameter that is very difficult to obtain analytically. As a result, its b-th moment was obtained. Using this conditional success probability analysis, the average AoI was investigated in both primary and secondary networks. Figure 9 shows the mean AoI for the hybrid, overlay and underlay modes. The packet is timelier from the tagged PR’s perspective in the overlay mode, since PTs hold exclusive access to channel usage with no interference from STs. Generally, the probability of re-transmission (a parameter that is proportional to the AoI) increases with an increase in θ_{Tr} provided that all other parameters remain unchanged. The AoI experience at the tagged SR reflects fewer channel access opportunities for STs due to PTs’ transmissions in the overlay mode. As a result, the AoI is higher at the tagged SR in the overlay model as presented in Figure 10. The hybrid model provides timely packets at the intending receiver from the tagged SR’s perspective.

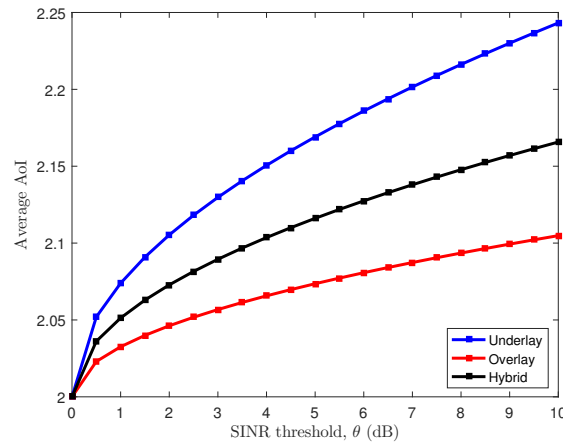


Figure 9. Average AoI in the primary network, ($\theta_p = 9.5$ dB, $v_p = v_s = 0.5$, $p_m = 0.2$, $\varepsilon = 0.25$).

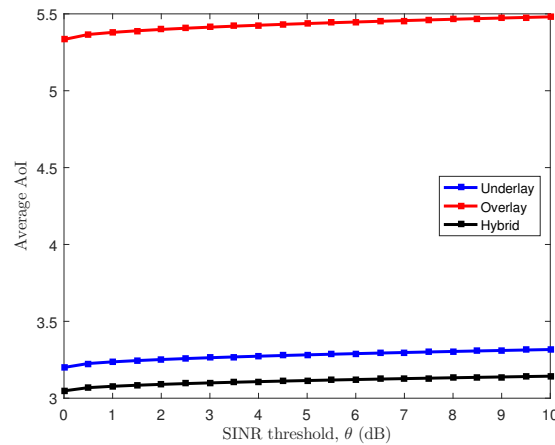


Figure 10. Average AoI in the secondary network, ($\theta_s = 9.5$ dB, $v_p = v_s = 0.5$, $p_m = 0.2$, $\varepsilon = 0.5$, $p_q = 0.25$, $p_f = 0.25$, $\rho = 0.2\varepsilon$).

6. Conclusions

The need to improve SUs's channel usage experience (i.e., transmission opportunities on the scarce spectrum resources), especially on channels where the presence of PUs may be dominant, means investigating users' performance under the hybrid spectrum access model becomes important. In this paper, we explored the performance of the hybrid spectrum access mode and compared it with overlay and underlay modes. We derived closed-form expressions for the selected metrics and demonstrated the ability of the hybrid spectrum access model to improve SUs channel access experience, while ensuring that the QoS of PUs is also satisfied. The obtained results showed that the hybrid spectrum access scheme can significantly improve the channel access experience of SUs without compromising the QoS constraints of PUs in massive cognitive networks. The analyses presented in this paper are useful in modeling the performance of large-scale CRN, where multiple PUs and SUs can access any channel concurrently. In the future, it may be interesting to obtain various detection probabilities conditioned on packet arrival and delivery rates. This may provide more insights regarding the performance of the hybrid spectrum access-based CRNs.

Author Contributions: Conceptualization, S.D.O. and B.T.M.; methodology, S.D.O.; software, S.D.O.; validation, S.D.O. and B.T.M.; resources, B.T.M.; writing—original draft preparation, S.D.O.; writing—review and editing, S.D.O. and B.T.M.; supervision, B.T.M.; funding acquisition, B.T.M. All authors have read and agreed to the published version of the manuscript.

Funding: This work was supported by the SENTECH Chair in Broadband Wireless Multimedia Communications (BWMC), Department of Electrical, Electronics, and Computer Engineering, University of Pretoria, South Africa.

Institutional Review Board Statement: Not applicable.

Informed Consent Statement: Not applicable.

Data Availability Statement: Not applicable.

Acknowledgments: The authors will like to appreciate the contributions of Attahiru S. Alfa to this research work.

Conflicts of Interest: The authors declare no conflict of interest.

References

1. Oh, J.; Choi, W. A hybrid cognitive radio system: A combination of underlay and overlay approaches. In Proceedings of the IEEE Vehicular Technology Conference-Fall, Ottawa, OT, Canada, 6–9 September 2010; pp. 1–5.
2. Okegbile, S. D.; Maharaj, B. T.; Alfa, A. S. Interference characterization in underlay cognitive networks with intra-network and inter-network dependence. *IEEE Trans. Mobile Comput.* **2020**. [[CrossRef](#)]
3. Zhao, Y.; Peng, M.; Liu, J. A Hybrid Spectrum Access Strategy with Channel Bonding and Classified Secondary User Mechanism in Multichannel Cognitive Radio Networks. *Sensors* **2019**, *19*, 4398. [[CrossRef](#)]
4. Zou, J.; Xiong, H.; Wang, D.; Chen, C. W. Optimal power allocation for hybrid overlay/underlay spectrum sharing in multiband cognitive radio networks. *IEEE Trans. Veh. Technol.* **2012**, *62*, 1827–1837. [[CrossRef](#)]
5. Song, H.; Hong, J. P.; Choi, W. On the optimal switching probability for a hybrid cognitive radio system. *IEEE Trans. Wirel. Commun.* **2013**, *12*, 1594–1605. [[CrossRef](#)]
6. Kaul, S.; Yates, R.; Gruteser, M. Real-time status: How often should one update? In Proceedings of the IEEE INFOCOM, Orlando, FL, USA, 25–30 March 2012; pp. 2731–2735.
7. Gu, Y.; Chen, H.; Zhai, C.; Li, Y.; Vucetic, B. Minimizing age of information in cognitive radio-based IoT systems: Underlay or overlay? *IEEE Internet Things J.* **2019**, *6*, 10273–10288. [[CrossRef](#)]
8. Leng, S.; Ni, X.; Yener, A. Age of information for wireless energy harvesting secondary users in cognitive radio networks. In Proceedings of the IEEE International Conference on Mobile Ad Hoc and Sensor Systems, Monterey, CA, USA, 4–7 November 2019; pp. 353–361.
9. Kosta, A.; Pappas, N.; Ephremides, A.; Angelakis, V. Age of information and throughput in a shared access network with heterogeneous traffic. In Proceedings of the IEEE Global Communications Conference, Abu Dhabi, UAE, 9–13 December 2018; pp. 1–6.
10. Mankar, P.D.; Abd-Elmagid, M.A.; Dhillon, H.S. Spatial distribution of the mean peak age of information in wireless networks. *arXiv* **2020**, arXiv:2006.00290.
11. Okegbile, S.D.; Maharaj, B.T.; Alfa, A.S. Outage and throughput analysis of cognitive users in underlay cognitive radio networks with handover. *IEEE Access* **2020**, *8*, 208045–208057. [[CrossRef](#)]
12. Okegbile, S.D.; Ogunranti, O.I. Users emulation attack management in massive internet of things enabled environment. *ICT Express* **2020**, *6*, 353–356. [[CrossRef](#)]
13. Okegbile, S.; Maharaj, B.; Alfa, A. Malicious users control and management in cognitive radio networks with priority queues. In Proceedings of the IEEE VTC Conference, Victoria, BC, Canada, 18 November–16 December 2020.
14. Okegbile, S.D.; Maharaj, B.T.; Alfa, A.S. Stochastic geometry approach towards interference management and control in cognitive radio network: A survey. *Comput. Commun.* **2021**, *166*, 174–195. [[CrossRef](#)]
15. Mankar, P.D.; Chen, Z.; Abd-Elmagid, M.A.; Pappas, N.; Dhillon, H.S. Throughput and Age of Information in a Cellular-based IoT Network. *arXiv* **2020**, arXiv:2005.09547.
16. Hu, Y.; Zhong, Y.; Zhang, W. Age of information in Poisson networks. In Proceedings of the IEEE International Conference on Wireless Communications and Signal Processing, Hangzhou, China, 29–31 July 2018; pp. 1–6.
17. Usman, M.; Koo, I. Access strategy for hybrid underlay–overlay cognitive radios with energy harvesting. *IEEE Sen. J.* **2014**, *14*, 3164–3173. [[CrossRef](#)]
18. Shaker, R.; Khakzad, H.; Taherpour, A.; Khattab, T.; Hasna, M.O. Hybrid underlay/overlay cognitive radio system with hierarchical modulation in the presence of channel estimation error. In Proceedings of the IEEE Global Communications Conference, Austin, TX, USA, 8–12 December 2014; pp. 967–972.
19. Jiang, X.; Wong, K.K.; Zhang, Y.; Edwards, D. On hybrid overlay–underlay dynamic spectrum access: Double-threshold energy detection and Markov model. *IEEE Trans. Veh. Technol.* **2013**, *62*, 4078–4083. [[CrossRef](#)]
20. Chen, Y.; Lei, Q.; Yuan, X. Resource allocation based on dynamic hybrid overlay/underlay for heterogeneous services of cognitive radio networks. *Wirel. Pers. Commun.* **2014**, *79*, 164–1664. [[CrossRef](#)]
21. Karmokar, A.K.; Senthuran, S.; Anpalagan, A. Physical layer-optimal and cross-layer channel access policies for hybrid overlay–underlay cognitive radio networks. *IET Commun.* **2014**, *8*, 266–2675. [[CrossRef](#)]

22. Bhowmick, A.; Prasad, B.; Roy, S.D.; Kundu, S. Performance of cognitive radio network with novel hybrid spectrum access schemes. *Wirel. Pers. Commun.* **2016**, *91*, 541–560. [[CrossRef](#)]
23. Duy, T.T.; Thanh, T.L.; Bao, V.N. A hybrid spectrum sharing approach in cognitive radio networks. In Proceedings of the IEEE International Conference on Computing, Management and Telecommunications, Da Nang, Vietnam, 27–29 April 2014; pp. 19–23.
24. Tefek U.; Lim, T. Interference management through exclusion zones in two-tier cognitive networks. *IEEE Trans. Wirel. Commun.* **2016**, *15*, 2292–2302 [[CrossRef](#)]
25. Baccelli, F.; Blaszczyzyn, B. *Stochastic Geometry and Wireless Networks, Volume I—Theory*; Now Publishers: Boston, MA, USA, 2010.
26. Okegbile, S.D.; Maharaj, B.T.; Alfa, A.S. Relaying techniques based outage analysis for mobile users in cognitive radio networks. In Proceedings of the IEEE Vehicular Technology Conference, Antwerp, Belgium, 25–28 May 2020; pp. 1–5.
27. Yang, H.H.; Arafa, A.; Quek, T.Q.; Poor, H.V. Locally adaptive scheduling policy for optimizing information freshness in wireless networks. In Proceedings of the IEEE Global Communications Conference, Waikoloa, HI, USA, 9–13 December 2019; pp. 1–6.
28. Okegbile, S.D.; Maharaj, B.T.; Alfa, A.S. Spatiotemporal Characterization of Users' Experience in Massive Cognitive Radio Networks. *IEEE Access* **2020**, *8*, 57114–57125. [[CrossRef](#)]
29. Haenggi, M.; Ganti, R.K. Interference in large wireless networks. *Found. Trends Netw.* **2008**, *3*, 127–248. [[CrossRef](#)]
30. Haenggi, M. The meta distribution of the SIR in Poisson bipolar and cellular networks. *IEEE Trans. Wirel. Commun.* **2015**, *15*, 2577–2589. [[CrossRef](#)]
31. Yang, H.H.; Quek, T.Q. Spatio-temporal analysis for SINR coverage in small cell networks. *IEEE Trans. Commun.* **2019**, *67*, 5520–5531. [[CrossRef](#)]
32. Yates, R.D.; Kaul, S.K. The age of information: Real-time status updating by multiple sources. *IEEE Trans. Inf. Theory* **2019**, *65*, 1807–1827. [[CrossRef](#)]
33. Chen, Z.; Pappas, N.; Bjornson, E.; Larsson, E.G. Age of information in a multiple access channel with heterogeneous traffic and an energy harvesting node. In Proceedings of the IEEE INFOCOM Workshops, Paris, France, 29 April–2 May 2019; pp. 662–667.